

Neural Langevin Dynamics: towards interpretable Neural Stochastic Differential Equations

Simon Koop, Mark Peletier, Jim Portegies, Vlado Menkovski

November 18, 2022

Abstract

Neural Stochastic Differential Equations (NSDE) have been trained as both Variational Autoencoders, and as GANs. However, the resulting Stochastic Differential Equations can be hard to interpret or analyse due to the generic nature of the drift and diffusion fields. By restricting our NSDE to be of the form of Langevin dynamics, and training it as a VAE, we obtain NSDEs that lend themselves to more elaborate analysis and to a wider range of visualisation techniques than a generic NSDE. More specifically, we obtain an energy landscape, the minima of which are in one-to-one correspondence with latent states underlying the used data. This not only allows us to detect states underlying the data dynamics in an unsupervised manner, but also to infer the distribution of time spent in each state according to the learned SDE. More in general, restricting an NSDE to Langevin dynamics enables the use of a large set of tools from computational molecular dynamics for the analysis of the obtained results.

1 Introduction

In recent years there has been widespread interest in Neural SDEs for generative modelling. Neural SDEs (NSDEs) learn the parameters in stochastic differential equations, which are natural extensions of ordinary differential equations to situations where uncertainty arises from many small and unobserved interactions, such as stock prices and molecular dynamics (Li et al., 2020; Kidger et al., 2021b). As such, Neural SDEs can be seen as incorporating uncertainty in Neural Ordinary Differential Equations.

NSDEs are said to combine the strengths of deep learning and classical modelling (Kidger et al., 2021b; Hasan et al., 2022). Deep learning brings performance and capacity, whereas classical modelling derives a lot of value from its interpretability. However, although from some perspective the dynamical system learned by an NSDE is itself a classical model, it is still a very complicated object, which makes it questionable whether NSDEs actually provide interpretability.

Indeed, what is often overlooked in Neural Differential Equation literature, is that finding the differential equation is only the start of the process. For interpretation, one needs to analyse stability, find stationary solutions, and analyse asymptotic behaviour, to name a few. In the particular case of NSDEs, one would want to find basins of attraction, as they could correspond to discrete states in the dynamics, would like to extract how long the system spends in each state and at what rates transitions occur. For general dynamical systems, these tasks are prohibitively complicated, which severely hampers interpretability.

To make NSDEs more interpretable, we introduce Neural Langevin Dynamics (NLD), in which we replace the generic vector field, which serves as the drift, by a gradient field, and let the system evolve by Langevin dynamics. This has the following advantages.

For one, there is a direct interpretation of “states” in the original system as the basins of attraction around local minima of the energy (e.g. (Lelièvre et al., 2010)) These local minima can be found using the vast toolbox of scalar optimisation methods — e.g. (Nocedal and Wright, 2006; Lee et al., 2016; Zhang and Li, 2021; Jin et al., 2017).

Sub-level sets of the energy function can then be used as approximations of the basins of attraction. This is illustrated by e.g. Figure 1, in which the contour lines clearly define regions that belong to specific states.

Moreover, transitions between local minima of the energy can be characterised in terms of mountain-pass connections between them. Such connections can be found using the numerical Mountain-Pass method (Choi and McKenna, 1993), also called String Method (E et al., 2002, 2005), and the corresponding transition rates can be estimated using Kramers’ formula (Kramers, 1940; Bovier et al., 2004; Landim et al., 2019).

Finally, there exist many more tools for visualising scalar functions than for visualising vector fields, aiding in the understanding by users of these models.

In this work, after introducing NLD in more detail, we show its potential and validity by training it as a Variational Autoencoder (VAE) on a pair of example problems. We show that the local minima indeed coincide with the true states underlying the data, and that information on relative occurrence of states can be extracted from the learned energy landscape.

Our results indicate that NLD allows us to extract interpretable information about the data dynamics, and in such a way that it opens up the use of tools from optimization and analysis, effectively providing a bridge between deep learning and classical modelling.

2 Related Work

(Tzen and Raginsky, 2019; Peluchetti and Favaro, 2020) view NSDEs as infinitely deep neural networks but don’t use them as time series models. (Kidger et al., 2021b) train their NSDE as a GAN instead of as a VAE. (Li et al., 2020; Kidger et al., 2021a) extend the so called adjoint sensitivity method to NSDEs and provide algorithms for storing Wiener processes. We do not use the adjoint sensitivity method but do use their algorithms for training NSDEs in the form of the torchsde package —<https://github.com/google-research/torchsde>. Moreover, (Li et al., 2020) introduce the training of an

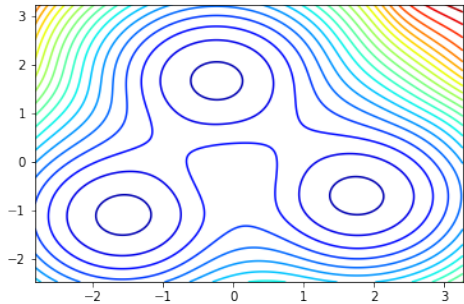


Figure 1: Contour of the energy landscape of an NLD model.

NSDE as a VAE on sequential data making them the most closely related to this work. (Hasan et al., 2022) also train NSDEs as VAEs but focus mostly on the dimensionality of the data space.

NSDEs can be viewed in the wider context of neural differential equations. The seminal paper in this area was (Chen et al., 2018). These were extended to models for sequential data in, among others (Rubanova et al., 2019; Kidger et al., 2020; Yildiz et al., 2019).

Moreover, NLD can be viewed in a line of physics inspired neural network models such as (Cranmer et al., 2020; Greydanus et al., 2019; Toth et al., 2020; Botev et al., 2021). The focus in the cited works however was more on performance and theoretical generalisability whereas our work focuses more on interpretability.

Langevin dynamics themselves have been extensively researched since the start of the 20th century and remain a topic of active research (Kramers, 1940; Berglund, 2011; Markowich and Villani, 2000). Besides their relevance for physical modelling, they play an important role in MCMC sampling see e.g. (Lelièvre et al., 2010).

3 Method

3.1 Neural Stochastic Differential Equations

In general, when training Neural Stochastic Differential Equations as Variational Auto-Encoders on some data $X = \{x = \{x_t\}_{t=0}^T\}$, one has two stochastic differential equations parameterising the prior $p_\theta(z)$ and approximate posterior $q_\varphi(z | x)$ distributions:

$$\begin{aligned}
 p_\theta(z) &\sim dz_t = h_\theta(z_t, t)dt + g_\theta(z_t, t)dW_t \\
 &\text{(prior),} \\
 q_\varphi(z | x) &\sim dz_t = f_\varphi(z_t, t, c_t)dt + g_\theta(z_t, t)dW_t \\
 &\text{(approximate posterior).}
 \end{aligned} \tag{1}$$

Here c_t is a function of the data x obtained by some encoder architecture, in this work a GRU. Throughout this work, c_t will only depend on $x_{s \leq t}$ so the models all operate in an

online fashion. The network being integrated against t , i.e. h_θ in the prior and f_φ in the approximate posterior, is called the drift, and the network being integrated against the Wiener Process, i.e. g_θ , is called the diffusion.

As shown in (Li et al., 2020), the Kullback-Leibler divergence between the approximate posterior and the prior is then given by

$$D_{KL}(q_\varphi(z|x) || p(z)) = \frac{1}{2} \int_0^T |u(z_t, t, c_t)|^2 dt,$$

$$g_\theta(z_t, t) u(z_t, t, c_t) = f_\varphi(z_t, t, c_t) - h_\theta(z_t, t),$$

where T is the final time.

Note that $p_\theta(z)$ is a learned distribution, parameterised by a neural network, representing the latent dynamics of the dataset as a whole. However, it is not easy to extract useful information about these latent dynamics from this representation of the distribution due to the generality of Equation (1).

3.2 Neural Langevin Dynamics

We introduce Neural Langevin Dynamics as a more interpretable alternative to NSDE. In NLD, we replace the drift h_θ in equation (1) by the scaled gradient of an energy $E_\theta : \mathbb{R}^d \rightarrow \mathbb{R}$ that is given by a neural network, and modify the evolution to either overdamped or underdamped Langevin dynamics.

In the case of overdamped Langevin dynamics, the prior and posterior evolutions are determined by

$$dz_t = -\gamma^{-1} \nabla_z E_\theta(z_t) dt + \sqrt{2\beta^{-1}\gamma^{-1}} dW_t$$

$$dz_t = -\gamma^{-1} \nabla_z E_\theta(z_t) dt$$

$$+ f_\varphi(z_t, t, c_t) dt + \sqrt{2\beta^{-1}\gamma^{-1}} dW_t$$

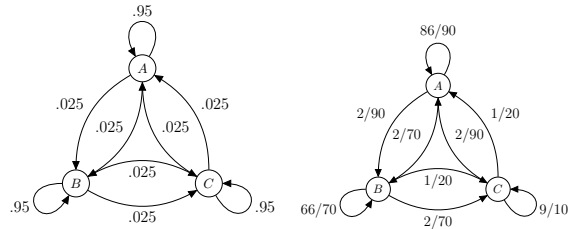
whereas in the case of underdamped Langevin dynamics, they are determined by

$$\begin{cases} dz_t^q = M^{-1} z_t^p dt \\ dz_t^p = [-\nabla E_\theta(z_t^q) - \gamma M^{-1} z_t^p] dt \\ \quad + \sqrt{2\gamma\beta^{-1}} dW_t \end{cases}$$

$$\begin{cases} dz_t^q = M^{-1} z_t^p dt \\ dz_t^p = -[\nabla E_\theta(z_t^q) + \gamma M^{-1} z_t^p] dt \\ \quad + f_\varphi(z_t^q, z_t^p, t, c_t) dt + \sqrt{2\gamma\beta^{-1}} dW_t. \end{cases}$$

Here, M is a positive diagonal matrix representing mass. The constants M, γ and β can either be fixed constants, or can be learned while training the model.

In the underdamped case, z^q plays the role of location, and z^p plays the role of momentum. Only the location, z^q should be used for decoding. Note that z^q follows a second-order stochastic differential equation.



(a) Graph for the first experiment. (b) Graph for the second experiment.

Figure 2: Graphs of the Markov processes underlying Experiment 1 and 2.

One of the great advantages of using Langevin dynamics is that this way, the SDE of the prior distribution has a known stationary distribution of the form

$$p_\infty(z) \sim \frac{\exp(-\beta E_\theta(z))}{\int_{\mathbb{R}^d} \exp(-\beta E_\theta(y)) dy}$$

in the overdamped case, and

$$p_\infty(z_q, z_p) \sim \frac{\exp(-\beta E_\theta(z_q))}{\int_{\mathbb{R}^d} \exp(-\beta E_\theta(y)) dy} \otimes \mathcal{N}(z_p; 0, M^{-1})$$

in the underdamped case. Due to ergodicity, the proportion of time spent in a region of the latent space, in the long run, corresponds to the mass attributed to that region by the stationary distribution, which only relies on the β and E_θ .

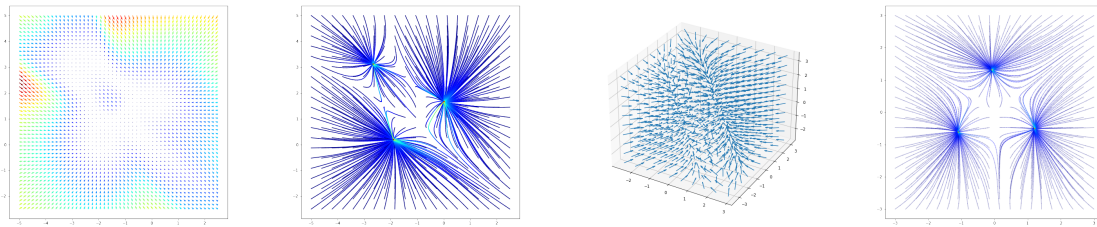
4 Experimental setup

We evaluate the capability of our method to develop an interpretable representation of data dynamics by training a model on data coming from a Markov chain. We then analyse the energy landscape of this model to recover the discrete states of the Markov chain and infer the time spent in each state.

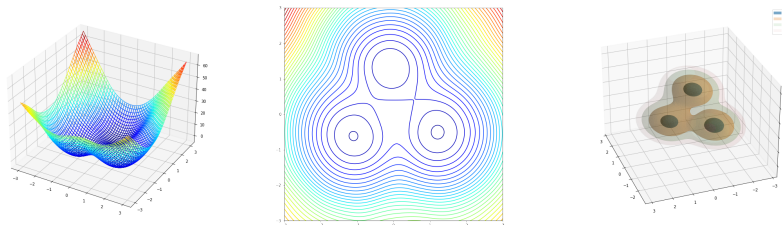
The data is generated as random-walks on a graph with three nodes. At each time step, a signal is emitted as a random vector sampled from a 15-dimensional multivariate normal distribution with mean and covariance matrix specified by the node the random walk is at.

For the first experiment, the transition probability from any state to any different state is 0.025 at each time step, resulting in a stationary distribution $(1/3, 1/3, 1/3)$, and an expected transition time of 20 time-steps. An overview of this is shown in Figure 2a.

For the second experiment, the transition probabilities are shown in Figure 2b. In this experiment, the stationary distribution is $(.45, .35, .2)$. This means that long time after initialisation, the system is expected to spend 45% of the time in state A , 35% in state B , and 20% of the time in state C .



(a) Quiver plot drift field. (b) Flow lines drift field. (c) Quiverplot of 3d drift field. (d) Projection of flow-lines starting in a 2d plane onto that same plane.



(e) A 3d plot of the energy landscape. (f) A contour plot of the energy landscape restricted to a plane through the three minima. (g) A 3d contour plot of the energy landscape through the three minima.

Figure 3: Visualisations of an NSDE (a-b) respectively an NLD (c-g) trained as a VAE on the data from experiment 1.

Code for both the generation of the datasets and the training of the models is provided in <https://anonymous.4open.science/r/dynvae-7F0D/>.

5 Visualisation advantages of NLD

Visualisation is an important tool for obtaining human knowledge in general, and can be useful for extracting knowledge from a trained model. To visualise trained models, if we only have a drift field, as is the case for a general NSDE, all we can really do is make a quiver plot of the drift field or plot the flow lines of the drift. For the two-dimensional case, this is shown in Figure 3a and Figure 3b.

As shown in Figure 3c, a quiver plot of a three-dimensional vector field is already rather hard to interpret. One can restrict these visualisation techniques to a plane to make them

more understandable, as is shown for a flow-line plot in Figure 3d.

If on the other hand the drift field of the model is a gradient field of an energy function, as is the case with the NLD models, we can visualise the the energy function directly. If the dimensionality of the vectorfield is too high to do this directly, we can restrict ourselves to a two-dimensional plane within the larger space, as is shown in Figure 3e and Figure 3f, or to a three-dimensional subspace, resulting in a visualisation like the one in Figure 3g.

These additional tools can aid a practitioner in interpreting what the model has learned and translating the obtained results to either existing or new knowledge about the data.

	From sampling (method a)	0 th order (method b)	2 nd order (method c)
Overdamped	0.047 ± 0.037	0.051 ± 0.022	0.040 ± 0.013
Underdamped	0.072 ± 0.068	0.041 ± 0.029	0.021 ± 0.0044

Table 1: ℓ^1 distance between estimated distribution of states and actual distribution of states in experiment 1.

	From sampling	0 th order	2 nd order
Overdamped	0.329 ± 0.013	0.322 ± 0.022	0.324 ± 0.017
Underdamped	0.335 ± 0.027	0.333 ± 0.011	0.336 ± 0.006

Table 2: First coordinate of the various estimations of the distribution of the state in experiment 1.

	mean accuracy	standard deviation
overdamped	$92.6\% \pm 0.6\%$	$1.6\% \pm 0.2\%$
underdamped	$82.2\% \pm 5.6\%$	$3.6\% \pm 1.4\%$

Table 3: Accuracy of unsupervised sequence segmentation for the same models as in Table 1

6 Results

We evaluate whether the learned energy landscape accurately represents the distribution of states underlying the data.

6.1 Experiment 1

In the first experiment the data-generating Markov chain has an invariant distribution of $(1/3, 1/3, 1/3)$, and we investigate whether this distribution can be recovered from the prior in the trained Neural Langevin Dynamics network.

We estimate the distribution of states in the learned prior in three different ways:

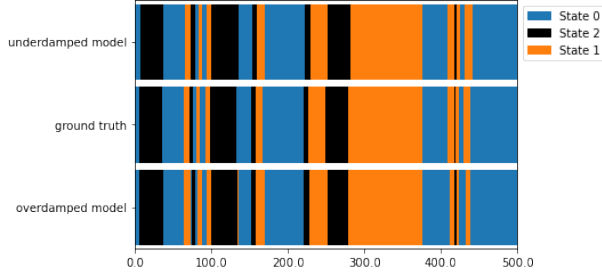


Figure 4: Results of unsupervised sequence segmentation of the first test sequence by both an underdamped and an overdamped NLD model.

- (a) by taking a thousand samples from the stationary distribution, performing gradient flow on them, and seeing what percentage of samples ends up in each well;
- (b) by taking the zeroth order approximation $f_i = \exp(-\beta E_\theta(x_i)) / \sum_j \exp(-\beta E_\theta(x_j))$ where f_i is the approximation of the size of the the well at x_i ;
- (c) by taking the second order approximation:

$$s_i = \alpha \frac{\exp(-\beta E_\theta(x_i))}{\rho_i},$$

$$\alpha = \left(\sum_j \frac{\exp(-\beta E_\theta(x_j))}{\rho_j} \right)^{-1},$$

$$\rho_i(x_i) = ((2\pi)^d \det(\beta^{-1} d^2 E_\theta(x_i)^{-1}))^{-1/2},$$

where $d^2 E_\theta(x_i)$ is the Hessian of the energy function at x_i , and d is the dimension of the latent space.

We report the ℓ^1 -distance to $(1/3, 1/3, 1/3)$ of each approximation for the top five best performing models ranked by second order approximation performance for both the underdamped and overdamped models in Table 1. For a more easily interpretable representation of the results, we also report the first coordinate of the learned distribution in Table 2.

	From sampling	0 th order	2 nd order
Underdamped	0.23 ± 0.040	0.24 ± 0.049	0.22 ± 0.0061

Table 4: ℓ^1 distance between estimated distribution of states and actual distribution of states in experiment 2.

A second question is whether the discovered states in the trained prior dynamics coincide with the ground-truth latent states in the data-generating Markov chain, and whether the trained encoder network successfully maps unseen incoming data to the latent states investigated above; this is a measure of the degree to which the training has managed to

	From sampling	0 th order	2 nd order
Coordinate 0	0.096 ± 0.014	0.090 ± 0.009	0.093 ± 0.003
Coordinate 1	0.373 ± 0.047	0.383 ± 0.053	0.379 ± 0.034
Coordinate 2	0.532 ± 0.041	0.527 ± 0.060	0.529 ± 0.033

Table 5: The distributions learned by the models from Table 4.

	mean accuracy	standard deviation
Underdamped	$85.3\% \pm 1.1\%$	$4.2\% \pm 0.3\%$

Table 6: Accuracy of unsupervised sequence segmentation for the same models as in Table 4

model the whole dynamics. We generated 500 test sequences from the same three-state Markov chain and mapped them to the latent space using the encoder of each of the models used for Table 1. Then we followed the gradient flow from each time step in each sequence of latent-space points to find out which well they belong to; this leads to a sequence of labels (0, 1, 2). To compare these labels to the ground truth, we selected the permutation of state labels (0, 1, 2) for which the overlap is maximised. We then computed the mean and standard deviation of the accuracy over the 500 sequences. The results are shown in Table 3.

Note that the models operate in an online fashion resulting in the encoded latent state lagging slightly behind the true latent state. Nonetheless, these results clearly show that the wells in the energy landscape coincide with the discrete states behind the data. Moreover, the models were trained on sequences of length 200, but are tested on sequences of length 500 and clearly generalise well.

6.2 Experiment 2

For the second experiment we restrict ourselves to underdamped models because those trained more stably in experiment 1. The distributions seem to represent the true distribution of the state much less accurately in this case, as shown in Table 4 and Table 5. This might be because these models were trained for much shorter due to time constraints.

In this experiment we tested on 500 test sequences of length 200. A visualisation of

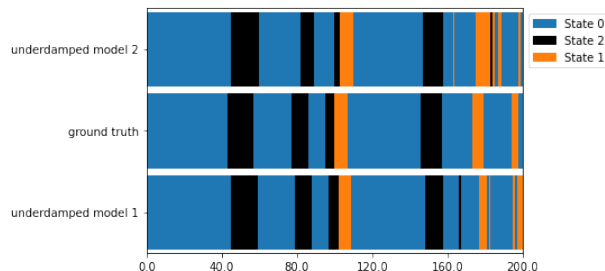


Figure 5: Results of unsupervised sequence segmentation by two models in experiment 2.

a segmented sequence in this experiment is given in Figure 5. The permutations found here correspond to a sorting of the distribution from high to low, indeed matching the stationary distribution $(.45, .35, .2)$ behind the true states. So as can be seen in Table 6, the local minima do still correspond to the states underlying the data.

7 Limitations and future research

Langevin dynamics can not represent periodic behaviour. Filtering out periodic signals can be a feature. However, when this behaviour is not wanted, another term needs to be introduced in the drift. The addition of a divergence-free rotation field to the drift might alleviate this problem without sacrificing the interpretability of the energy landscape.

We had some trouble getting our NLD models to train consistently: the loss would become NaNs or jump several orders of magnitude. We conjecture that this is due to poor choice of hyper-parameters and architecture, since we encountered the same problems with the NSDE models we trained on the same data. Nonetheless, more work needs to be put into getting these models to train consistently.

8 Conclusion

To provide a more interpretable alternative to Neural Stochastic Differential Equations, we introduce Neural Langevin Dynamics, in which we replace the general drift term by the gradient of a trainable energy and let the system evolve by Langevin dynamics. The gain in interpretability comes both from the better options for visualisations of scalar functions over general vectors fields, and the better options for downstream processing in the form of classical methods from optimisation and analysis. With these methods, we can extract important properties such as stationary distributions and discrete states. When we apply NLD to example problems, it recovers the discrete states underlying the data. These results show promise that NLD is able to combine the performance of neural networks with the interpretability of classical differential equation based models.

Bibliography

- Nils Berglund. Kramers' law: Validity, derivations and generalisations. *arXiv preprint arXiv:1106.5799*, 2011.
- Aleksandar Botev, Andrew Jaegle, Peter Wirnsberger, Daniel Hennes, and Irina Higgins. Which priors matter? benchmarking models for learning latent dynamics. *NeurIPS 2021 Track Datasets and Benchmarks*, November 2021.
- Anton Bovier, Michael Eckhoff, Véronique Gayrard, and Markus Klein. Metastability in reversible diffusion processes i: Sharp asymptotics for capacities and exit times. *Journal of the European Mathematical Society*, 6(4):399–424, 2004.

- Ricky TQ Chen, Yulia Rubanova, Jesse Bettencourt, and David K Duvenaud. Neural ordinary differential equations. *Advances in neural information processing systems*, 31, 2018.
- Yung Sze Choi and P Joseph McKenna. A mountain pass method for the numerical solution of semilinear elliptic problems. *Nonlinear Analysis: Theory, Methods & Applications*, 20(4):417–437, 1993.
- Miles Cranmer, Sam Greydanus, Stephan Hoyer, Peter Battaglia, Spergel David, and Shirley Ho. Lagrangian neural networks. *ICLR 2020 Workshop DeepDiffEq*, 2020.
- Weinan E, Weiqing Ren, and Eric Vanden-Eijnden. String method for the study of rare events. *Physical Review B*, 66(5):052301, 2002.
- Weinan E, W. Ren, and E. Vanden-Eijnden. Finite temperature string method for the study of rare events. *Journal of Physical Chemistry B*, 109(14):6688–6693, 2005.
- Sam Greydanus, Misko Dzamba, and Jason Yosinski. Hamiltonian neural networks. *NeurIPS 2019*, 2019.
- Ali Hasan, Joao M. Pereira, Sina Farsiu, and Vahid Tarokh. Identifying latent stochastic differential equations. *IEEE Transactions on Signal Processing*, 70:89–104, 2022. ISSN 1941-0476. doi: 10.1109/tsp.2021.3131723. URL <http://dx.doi.org/10.1109/tsp.2021.3131723>.
- Chi Jin, Rong Ge, Praneeth Netrapalli, Sham M Kakade, and Michael I Jordan. How to escape saddle points efficiently. In *International Conference on Machine Learning*, pages 1724–1732. PMLR, 2017.
- Patrick Kidger, James Morrill, James Foster, and Terry Lyons. Neural controlled differential equations for irregular time series. *Advances in Neural Information Processing Systems*, 33:6696–6707, 2020.
- Patrick Kidger, James Foster, Xuechen Li, and Terry Lyons. Efficient and accurate gradients for neural sdes, 2021a.
- Patrick Kidger, James Foster, Xuechen Li, and Terry J Lyons. Neural sdes as infinite-dimensional gans. In Marina Meila and Tong Zhang, editors, *Proceedings of the 38th International Conference on Machine Learning*, volume 139 of *Proceedings of Machine Learning Research*, pages 5453–5463. PMLR, 18–24 Jul 2021b. URL <https://proceedings.mlr.press/v139/kidger21b.html>.
- H. A. Kramers. Brownian motion in a field of force and the diffusion model of chemical reactions. *Physica*, 7(4):284–304, 1940.

- Claudio Landim, Mauro Mariani, and Insuk Seo. Dirichlet’s and Thomson’s principles for non-selfadjoint elliptic operators with application to non-reversible metastable diffusion processes. *Archive for rational mechanics and analysis*, 231(2):887–938, 2019.
- Jason D Lee, Max Simchowitz, Michael I Jordan, and Benjamin Recht. Gradient descent only converges to minimizers. In *Conference on learning theory*, pages 1246–1257. PMLR, 2016.
- Tony. Lelièvre, Gabriel. Stoltz, and Mathias Rousset. *Free energy computations : a mathematical perspective*. Imperial College Press, London ;, 2010.
- Xuechen Li, Ting-Kam Leonard Wong, Ricky T. Q. Chen, and David Duvenaud. Scalable gradients for stochastic differential equations. In Silvia Chiappa and Roberto Calandra, editors, *Proceedings of the Twenty Third International Conference on Artificial Intelligence and Statistics*, volume 108 of *Proceedings of Machine Learning Research*, pages 3870–3882. PMLR, 26–28 Aug 2020. URL <https://proceedings.mlr.press/v108/li20i.html>.
- Peter A Markowich and Cédric Villani. On the trend to equilibrium for the fokker-planck equation: an interplay between physics and functional analysis. *Mat. Contemp*, 19:1–29, 2000.
- Jorge Nocedal and Stephen J Wright. *Numerical optimization*. Springer Series in Operation Research and Financial Engineering. 2nd edition, 2006.
- Stefano Peluchetti and Stefano Favaro. Infinitely deep neural networks as diffusion processes. In Silvia Chiappa and Roberto Calandra, editors, *Proceedings of the Twenty Third International Conference on Artificial Intelligence and Statistics*, volume 108 of *Proceedings of Machine Learning Research*, pages 1126–1136. PMLR, 26–28 Aug 2020. URL <https://proceedings.mlr.press/v108/peluchetti20a.html>.
- Yulia Rubanova, Ricky T.Q. Chen, and David Duvenaud. Latent odes for irregularly-sampled time series. *NeurIPS 2019*, 2019.
- Peter Toth, Danilo J. Rezende, Andrew Jaegle, Sébastien Racanière, Aleksandar Botev, and Irina Higgins. Hamiltonian generative networks. 2020.
- Belinda Tzen and Maxim Raginsky. Neural stochastic differential equations: Deep latent gaussian models in the diffusion limit. *arXiv preprint arXiv:1905.09883*, 2019.
- Cagatay Yildiz, Markus Heinonen, and Harri Lahdesmaki. Ode2vae: Deep generative second order odes with bayesian neural networks. *Advances in Neural Information Processing Systems*, 32, 2019.
- Chenyi Zhang and Tongyang Li. Escape saddle points by a simple gradient-descent based algorithm. *Advances in Neural Information Processing Systems*, 34:8545–8556, 2021.